Regulation of Root Elongation under Phosphorus Stress Involves Changes in Ethylene Responsiveness[1]

Zhong Ma, Tobias I. Baskin, Kathleen M. Brown, and Jonathan P. Lynch*

Department of Horticulture, The Pennsylvania State University, 103 Tyson Building, University Park, Pennsylvania 16802 (Z.M., K.M.B., J.P.L.); and Division of Biological Sciences, University of Missouri, Columbia, Missouri 65211–7400 (T.I.B.)

We characterized the growth of the primary root of Arabidopsis under phosphorus sufficiency (1 mM phosphate) and deficiency (1 μM phosphate), focusing on the role of ethylene. We quantified the spatial profile of relative elongation with a novel method based on image processing, as well as the production rates of cortical cells, trichoblasts, and atrichoblasts. Phosphorus deficiency moderately decreased the maximal rate of relative elongation, shortened the growth zone, and decreased the production rate of both epidermal cell types but not of cortical cells. Inhibiting ethylene production (with aminoethoxyvinyl-glycine) or action (with 1-methylcyclopropene) increased elongation in high phosphorus and decreased it in low phosphorus. That these effects were specific to ethylene was confirmed by negating the effect of inhibited ethylene production with simultaneous treatment with an ethylene precursor (1-aminocyclopropane-1-carboxylic acid). Under both phosphorus regimes, ethylene regulated the maximal rate of relative elongation rather than the size of the growth zone. In addition, inhibiting ethylene action in high versus low phosphorus elicited opposite responses for the position of root hair initiation and for the production rates of cortex cells and atrichoblasts. We conclude that the root system acclimates to phosphorus deficiency by changing the signal transduction pathway connecting ethylene levels to growth and division.

Plant root systems display an array of physiological, morphological, and architectural responses to low phosphorus availability. These responses enhance the ability of the root to explore the soil and include changes in branching patterns, in elongation rate, and in root hair length and density (Bates and Lynch, 1996; Bonser et al., 1996; Borch et al., 1999; Lynch and Brown, 2001; Ma et al., 2001a). These changes accompany changes in biochemical and metabolic processes and both together presumably represent adaptive responses to assist growth during phosphorus deficiency. In particular, the growth of root hairs and their response to phosphorus availability is important in the acquisition of this highly immobile nutrient (Lewis and Quirk, 1967; Bhat and Nye, 1974; Gahoonia and Nielsen, 1997; Bates and Lynch, 2000a, 2000b; Ma et al., 2001b).

In response to low phosphorus, adaptive changes in roots may be mediated through the plant hormone ethylene. Both phosphorus deficiency and ethylene cause similar changes in root systems, such as aerenchyma formation, altered root growth angle, and stimulated root hair development (He et al., 1992; Lynch and Brown, 1997; Borch et al., 1999; Lynch and Brown, 2001). In bean (*Phaseolus vulgaris*), ethylene inhibits root elongation in phosphorus-sufficient conditions but maintains elongation under phosphorus deficiency (Borch et al., 1999). This finding suggests that roots respond to phosphorus stress by changing ethylene signal transduction pathways involved in regulating growth.

In this report, we focus on the role of ethylene in mediating growth responses to low phosphorus availability, characterizing the spatial profile of relative elongation rate. Although root length has been measured in Arabidopsis grown at various levels of phosphorus (Bates and Lynch, 1996; Williamson et al., 2001; López-Bucio et al., 2002), root length reflects the overall elongation rate, a parameter that comprises several components, any of which may be regulated specifically to change growth rate. These components include the length of the growth zone, the maximal rate of elongation, the shape of the spatial profile, and the magnitude of elongation within the meristem. Parameters of this kind are presumably closer to the output of a signal transduction cascade, so by quantifying elongation in this way, we will be better able to understand how growth and ethylene responsiveness are linked under low phosphorus.

The spatial profile of relative expansion is obtained from the derivative of the spatial profile of velocity, the speed at which each point on the root surface moves forward. A point moves forward based on the expansion of the region of the root between it and the base of the growth zone: A point at the very tip moves forward rapidly propelled by the expansion of

[1] This work was supported in part by Binational Agricultural Research and Development Fund (to J.P.L. and K.M.B.), by the U.S. Department of Agriculture/National Research Initiative (grant no. 9900632 to J.P.L. and K.M.B.), and by the National Science Foundation (award no. IBN 9817132 to T.I.B.).

* Corresponding author: e-mail JPL4@psu.edu; fax 814–863–6139.

Article, publication date, and citation information can be found at www.plantphysiol.org/cgi/doi/10.1104/pp.012161.

the entire growth zone behind it; a point in the mature zone is motionless because there is no growth behind it; and points in between move at rates decreasing from tip to base along with the decreasing portion of growth zone they surmount. The velocity would decrease linearly from tip to base if all elements within the growth zone elongated at the same relative rate; in real roots, differences between regions in relative elongation rate give rise to profiles of velocity that are more complex. With the velocity profile known, its derivative gives the local elongation behavior required to produce that profile.

To obtain the velocity profile of a growing root, scientists have marked roots with various materials, such as ink or graphite particles, and have measured the displacement of the marks over time manually (Sharp et al., 1988; Beemster and Baskin, 1998; Muller et al., 1998). Marking frequently inhibits root growth, and it is difficult to place more than a few marks within the growth zone. In addition, measurable displacements require long time intervals between images, and the subsequent manual tracking of the marks is tedious, subjective, and noisy. To overcome these limitations, investigators are turning to methods from image processing, where velocity is recovered algorithmically. In these methods, a stack or image sequence is obtained and treated as a single, three-dimensional image volume. Within the volume, features within the volume that are parallel to the time axis have zero velocity, and the angle to the time axis of moving features defines the speed of motion. Such methods are straightforward for rigid objects, but they are much more complex for a deformable object such as a growing plant organ. Nevertheless, such techniques have been applied to leaf growth (Schmundt et al., 1998), and an algorithm has been developed specifically for roots, which recovers the spatial distribution of velocity at high spatial and temporal resolution (Jiang, 2001; Van der Weele, 2001). The algorithm uses a stack of nine images with 10 s between each and provides a reliable velocity at most pixels of the image, equivalent to about 1 μm in our conditions.

We have used this method to characterize the spatial profile of relative elongation rate throughout the growth zone of roots grown under sufficient and low phosphorus conditions and in the presence or absence of inhibitors of ethylene. In addition, we have quantified the time and place where root hairs emerged and the rate of production of cortex and epidermal cells because these parameters too are likely to offer insight into how the root responds to low phosphorus and the role therein of ethylene.

RESULTS

Root Elongation Rate over Time

For phosphorus deficiency, we used 1 μM phosphate and for sufficiency, 1 mM phosphate. Although 1 mM phosphate is more than roots usually encounter in nature, it is optimal for primary root growth of Arabidopsis in unbuffered media, as employed here (T.I. Baskin, unpublished data; see also López-Bucio et al., 2002). The Arabidopsis primary root elongated at a steady rate over time, under both high and low phosphorus, and the average growth rate was reduced by about 30% under low phosphorus (Fig. 1).

To determine the role of ethylene in root responses to phosphorus availability, seeds were germinated on high or low phosphorus medium, and on the 6th d after germination they were exposed to the ethylene action inhibitor 1-methylcyclopropene (MCP). For plants grown at high phosphorus, root elongation rate increased during the 1st d of treatment and remained constant thereafter; whereas for plants grown at low phosphorus, MCP treatment decreased root elongation within a few days, with the greatest decrease happening during the 4th d of treatment (Fig. 1; Table I). Under high phosphorus, the higher MCP dose was clearly more effective than the lower dose, but under low phosphorus, the higher MCP dose was only slightly more effective.

To confirm that the effects of MCP result from inhibiting ethylene, we used an inhibitor of ethylene biosynthesis, aminoethoxyvinyl-Gly (AVG). This inhibitor, like MCP, stimulated root growth under phosphorus sufficiency and inhibited it under deficiency (Fig. 2). To confirm that AVG acted through inhibiting ethylene synthesis, we added ethylene back to these treatments by incorporating the precursor 1-aminocyclopropane-1-carboxylic acid (ACC) into the medium. At 0.2 μM, ACC restored the elongation rate to nearly the level for high phosphorus alone and to exactly the level for low phosphorus (Fig. 2). Higher doses of ACC, around 1 μM, reduced root elongation rate in both phosphorus treatments and apparently more effectively under phosphorus deficiency. These results confirm in Arabidopsis the previous findings in bean, namely that under phosphorus sufficiency, ethylene limits elongation but

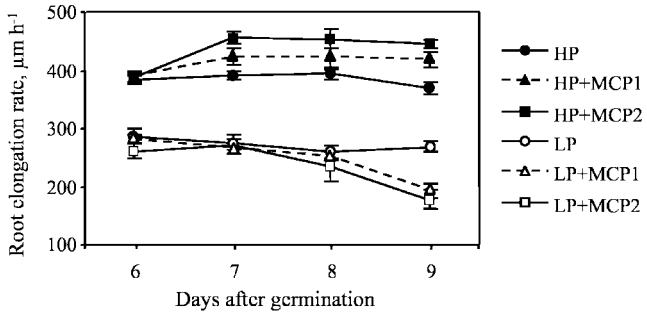

Figure 1. Time course of primary root elongation for Arabidopsis plants grown on either high (1 mM) or low (1 μM) phosphorus medium. MCP treatments were started at d 6 after germination. MCP1 = 23.3 nL L^{-1} MCP gas, and MCP2 = 93.1 nL L^{-1} MCP gas. Data are means ± SE of six plates, with three to four seedlings per plate.

Table I. *ANOVA for data presented in the figures*

Parameter	Statistics	*P*	MCP	*P* × MCP
Root elongation rate	*F* value	433.9	0.45	35.78
	Pr > *F*	<0.0001	ns[a]	<0.0001
Strain in the meristem	*F* value	0.71	0.78	0.76
	Pr > *F*	ns	ns	ns
Maximal strain	*F* value	146.8	1.01	23.04
	Pr > *F*	<0.0001	ns	<0.0001
Location of the maximal strain	*F* value	7.5	17.01	21.33
	Pr > *F*	0.0113	<0.0001	<0.0001
Meristem length	*F* value	1.01	0.15	0.18
	Pr > *F*	ns	ns	ns
Elongation zone length	*F* value	35.11	0.98	0.52
	Pr > *F*	<0.0001	ns	ns
Growth zone length	*F* value	42.74	1.46	0.41
	Pr > *F*	<0.0001	ns	ns
Trichoblast length	*F* value	394	31.23	91.17
	Pr > *F*	<0.0001	<0.0001	<0.0001
Atrichoblast length	*F* value	117.4	15.3	32.42
	Pr > *F*	<0.0001	0.0002	<0.0001
Cortical cell length	*F* value	569.2	55.59	11.38
	Pr > *F*	<0.0001	<0.0001	0.001
Trichoblast flux	*F* value	37.1	6.16	1.6
	Pr > *F*	<0.0001	0.0112	ns
Atrichoblast flux	*F* value	80.6	3.39	2.85
	Pr > *F*	<0.0001	0.0308	0.0391
Cortical cell flux	*F* value	14.9	8.21	5.06
	Pr > *F*	0.0015	0.0039	0.0209
First hair initiation	*F* value	310.5	3.5	20.22
	Pr > *F*	<0.0001	0.0456	<0.0001
First hair to the end of growth zone	*F* value	26.5	4.8	8.85
	Pr > *F*	<0.0001	0.02	0.0021

[a] ns, No significant difference at $P < 0.05$.

that ethylene maintains root elongation under phosphorus limitation.

Analysis of the Profiles of Velocity and Relative Elongation Rate

In high and low phosphorus treatments, neither the spatial distribution of velocity nor the mature cell length differed significantly on d 5, 7, and 9 after plating (data not shown), signifying steady-state growth. Therefore, data from d 9 are presented for all treatments.

An example of a velocity profile obtained with the new algorithm is shown in Figure 3A. The example is for a root growing under phosphorus-sufficient conditions, but the characteristics of the profiles were similar for all treatments and roots. In the first few hundred microns from the quiescent center (i.e. $x = 0$), velocity increased gradually with position. This gradual increase was followed by an abrupt transition to a region where velocity increased steeply with position. The increase in velocity eventually slowed, and velocity became constant. In the following analysis, we refer to the region where velocity increased gradually as the meristem and use the position of the abrupt transition to define the end of the meristem. In preliminary experiments, this position has been

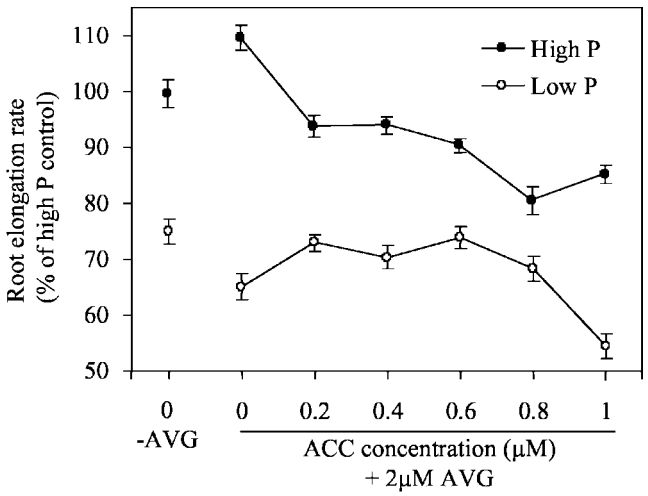

Figure 2. Root elongation rate on high (1,000 μM) and low (1 μM) phosphorus media in the presence or absence of 2 μM AVG and ACC, as indicated. Plants germinated on high or low phosphorus medium and treatments with AVG (2 μM) and ACC initiated on d 6 after germination. Elongation rates are reported for d 3 of treatment (9 d after germination). Data are means ± SE of six plates, with three to four seedlings per plate.

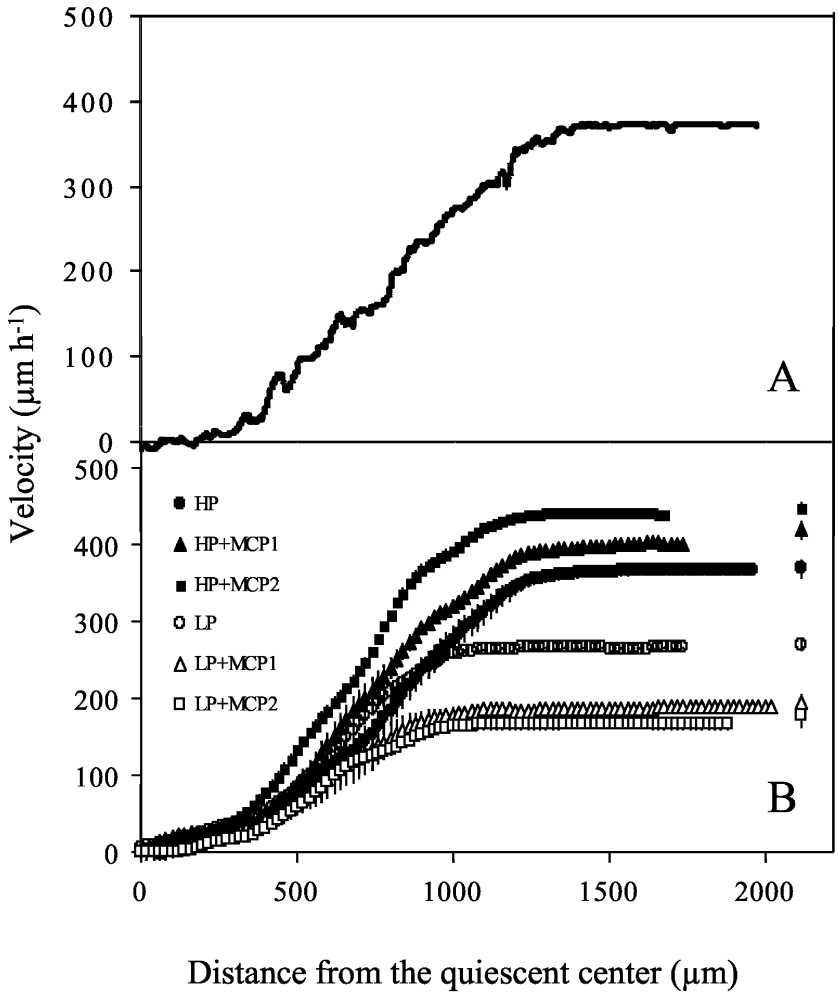

Figure 3. Profiles of velocity versus distance from the quiescent center for the primary root of 9-d-old Arabidopsis plants. Treatments as for Figure 1. A, An example of a raw velocity profile for a single root (high-phosphorus treatment). B, Average velocity profiles. Raw velocity profiles for each root were smoothed and interpolated as described in "Materials and Methods." Data points are means from six roots ± SE, shown when larger than symbols. For clarity, data points are shown every 20 μm, but actual data were collected every 1 μm. Symbols near the right *y* axis represent average final velocity at d 9, taken from Figure 1, which were measured on roots of a different set of plants than those used for imaging and kinematic analysis.

mapped close to the position where cell division stops (C.M. Van der Weele, V.B. Ivanov, and T.I. Baskin, unpublished data).

To compare velocity profiles between treatments, the raw data were smoothed and interpolated to 1-μm intervals by the piecewise, iterative procedure used previously (Beemster and Baskin, 1998). These data were then averaged over the roots in a given treatment (Fig. 3B). The reproducibility among roots is evident from the small size of the SEs of the six replicate observations. In addition, the final velocity determined through imaging was indistinguishable from velocity determined for a different set of roots by marking the plates (Fig. 3B, symbols to the right of each curve), showing that the brief removal of the plate from the chamber for imaging (6 min) did not alter the growth behavior detectably.

To examine relative elongation rate, the smoothed velocity data were differentiated for each root and then averaged over the roots in a treatment (Fig. 4). There was a region of relatively low and steady relative elongation rate in the apical few hundred microns of the root. After that, elongation rate rose to a peak and then declined to zero; however, the peak was not reached smoothly but instead was flanked by shoulders where elongation rate was roughly constant with position. These features were robust to different curve-fitting procedures (data not shown) and may indicate an inherent oscillatory character to growth within the root. Despite the complex shapes, the profiles appeared qualitatively similar in all treatments. Comparing high and low phosphorus, the major difference appeared to be the size of the zone of elongation (Fig. 4A); whereas ethylene inhibition appeared to affect the overall magnitude of the elongation rate (Fig. 4B).

As a supplement to polynomial fits, we also fitted the raw velocity data from each root to a model consisting of two lines joined at a breakpoint, excluding the region basal of the growth zone where velocity is constant. The breakpoint was used to divide the growth zone into meristem and elongation zone, and the slopes were used to estimate an average relative elongation rate for each of the two regions. No treatment significantly changed the length or the rate of relative elongation of the meristem (Figs. 5 and 6), showing that the meristem is involved scarcely if at all in growth responses to phosphorus or ethylene. In

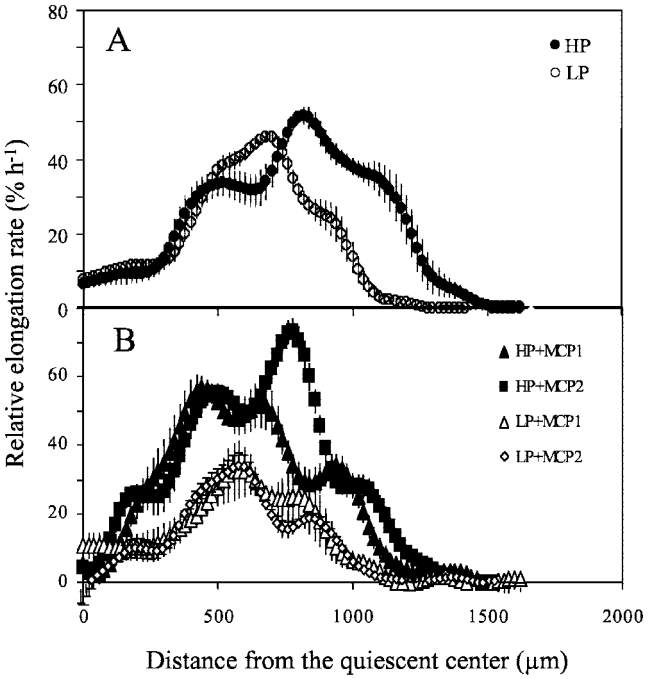

Figure 4. Profiles of relative elongation rate versus distance from the quiescent center for the primary root of 9-d-old Arabidopsis plants. Treatments as for Figure 1. Data points are means from six roots ± SE. For clarity, data points are shown every 20 μm, but actual data were collected every 1 μm.

the elongation zone, low phosphorus reduced both average and maximal relative elongation rate as well as the length of the zone. Inhibiting ethylene affected average and maximal relative elongation rate, enhancing the difference between high and low phosphorus, but mostly did not affect the size of the growth zone. Our results show that during the growth response of roots to low phosphorus, ethylene does not appear to be involved in maintaining the size of the growth zone but is required to maintain relative elongation rates throughout the zone of elongation.

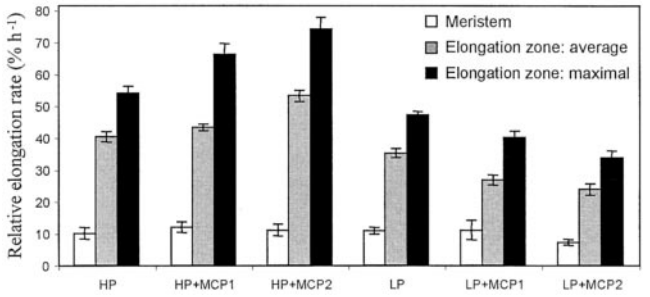

Figure 5. Relative elongation rate in the meristem and zone of elongation in the primary root of 9-d-old Arabidopsis plants. Maximal elongation rate is the peak value from the polynomial fits; average elongation rate is obtained from the linear fit to the velocity within the elongation zone; meristem elongation rate is obtained from the linear fit to the velocity within the elongation zone. Treatments as for Figure 1. Bars are means from six roots ± SE.

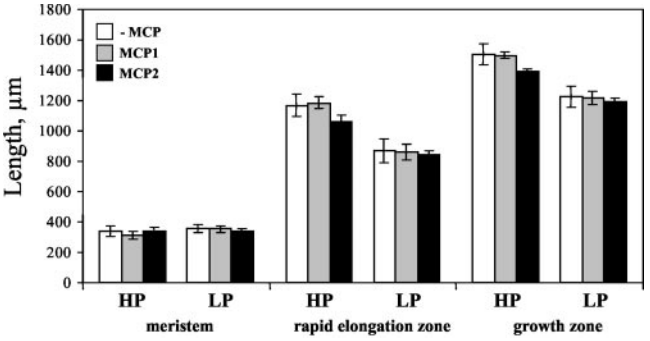

Figure 6. Partition of the growth zone showing the estimated size of the meristem, the length of the entire growth zone, and the approximate size of the rapid elongation zone defined as the difference between the previous two regions. Treatments as for Figure 1. Bars are means from six roots ±SE.

Cell Length and Cell Flux

To gain further insight into the growth changes under phosphorus deficiency, we measured the mature cell length of cortical and epidermal cells (trichoblasts and atrichoblasts) and calculated cell flux into the mature zone, a parameter that at steady-state growth is equal to the rate of cells produced by the meristem, per file. In phosphorus-sufficient conditions, all cell types were the same length and consequently were produced at the same rate (Fig. 7). Under these conditions, when ethylene was inhibited by MCP, cortical and atrichoblast cell lengths changed in parallel with elongation rate so that cell flux was little affected, a finding that shows that removing ethylene action stimulates the elongation

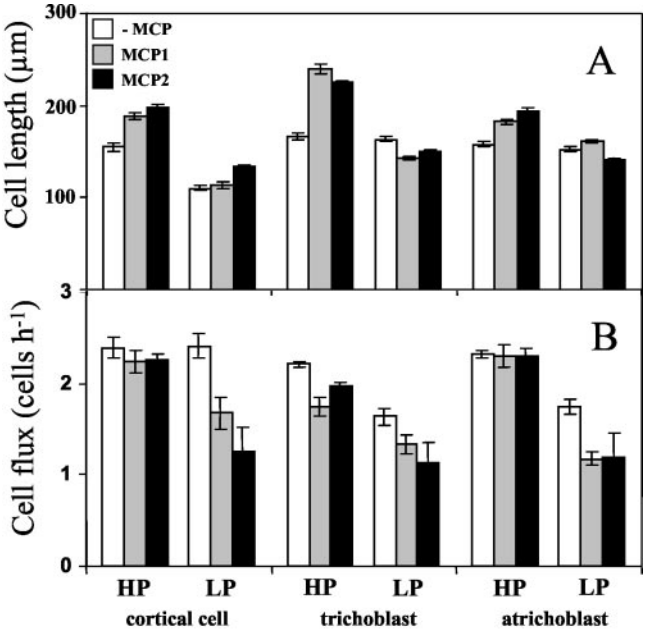

Figure 7. Effect of phosphorus and ethylene inhibition on cell length (A) and cell flux (B) of different cell types from Arabidopsis roots. Treatments as for Figure 1. Bars are means from six roots ± SE.

of phosphorus-sufficient roots without stimulating cell production. In fact, the flux of trichoblast cells was reduced, and their lengths became significantly longer than atrichoblasts or cortical cells.

Under phosphorus deficiency, the uniformity among the tissues in cell length was lost, and cortical cells became shorter than the other two cell types (Fig. 7). The diminished cortical cell length reflected the reduced elongation rate, with no change in the production rate of cortical cells. In contrast, both epidermal cell types were produced more slowly, and they were similar in length to phosphorus-sufficient roots, which may reflect an adaptation to preserve epidermal cell length. With inhibition of ethylene, cell flux was sharply reduced in all tissues, indicating that under phosphorus deficiency, ethylene is involved in maintaining not only elongation but also cell production.

Root Hair Initiation

Under phosphorus deficiency, the point of root hair initiation was closer to the quiescent center; however, this change was roughly proportional to the change in the size of the growth zone so that distance between the first hair and the end of the growth zone was little altered by the stress (Fig. 8). Like relative elongation, the response of the location of root hair initiation to the inhibition of ethylene action depended on phosphorus availability. At high phosphorus availability, root hairs initiated progressively farther from the tip, and because the size of the growth zone was little changed, at the higher concentration of MCP root hairs initiated actually basal of the point where growth stopped; whereas at low phosphorus with ethylene action inhibited, root hairs initiated closer to the tip and farther from the end of the growth zone.

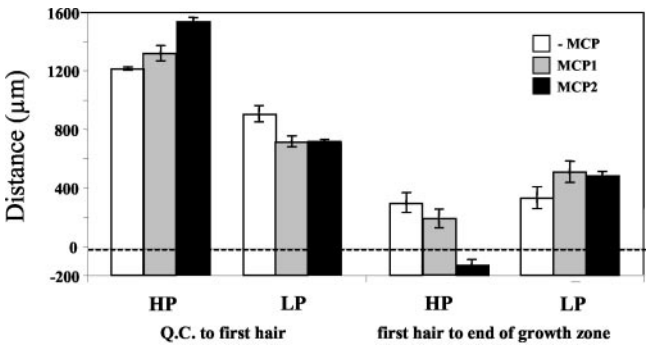

Figure 8. The effect of phosphorus and ethylene inhibition on the position of root hair initiation as measured by the distance between the quiescent center (Q.C.) to the location of the first root hair, and the distance between the first root hair and the point where root hairs began to mature. Treatments as for Figure 1. Bars are means from six roots ± SE.

DISCUSSION

To characterize how the Arabidopsis root responds to phosphorus deficiency, we grew plants in agar medium in petri dishes because this arrangement is convenient for quantifying root growth. In contrast to other studies of Arabidopsis roots in agar media, which report that primary root elongation accelerates over time (e.g., Beemster and Baskin, 1998), root elongation rate was fairly steady under our experimental conditions (Fig. 1). The steady elongation rate may reflect the fact that in our studies, roots grew inside the medium at a 45° angle, rather than as in other studies nearly vertically on the surface of the medium. Our root growth environment is arguably more similar to soil, because the medium provides some mechanical impedance. In addition, unlike earlier studies, we did not use Suc in the growth media. Note that the absolute growth rates that we observed (approximately 1 cm d^{-1}) exceed those of many published reports, showing that our system permits vigorous root growth.

To characterize the spatial profile of elongation rate within the root, we measured the spatial profile of velocity. For all treatments, velocity profiles had three distinct domains: a gradual linear increase in the meristematic region, then a sharp transition to steeper linear increase in the elongation zone, followed by a second transition to a constant velocity value (Fig. 3). These profiles contrast with those reported previously for roots, including Arabidopsis, which show velocity increasing sigmoidally with distance from the tip (e.g., Erickson and Sax, 1956; Beemster and Baskin, 1998). The reason for this difference is not clear. It is unlikely to be explained by growth within the agar because roots growing on the surface of the agar and analyzed with the same algorithm show a similar pattern (Van der Weele, 2001). The previous studies may have smoothed out the linear character of the velocity profile because the imaging time required was at least 10 times that used here. In any case, the use of a model containing two lines joined at a breakpoint usefully supplemented the polynomial fits because the breakpoint divided the growth zone into elongation zone and meristem analytically, and the slopes of the regression lines provided a robust estimate of the average relative elongation rate for each region. The linear fit has been validated by analysis of residuals that shows no systematic departure from the model except for the end of the second slope, where growth is stopping (Van der Weele, 2001).

For both phosphorus treatments, the relative elongation rate profile obtained by the polynomial fits followed a roughly bell-shaped curve with a small amount of wobbling. Because this rate is calculated by taking the first derivative of a set of polynomials fitted to the raw data, the profile can only be an approximation, and the degree to which it reflects real growth phenomena is subject to the extent of

either over-smoothing or under-smoothing of the velocity profile. We took care in choosing the optimal interval for curve fitting, and we consider that the wobbling in the curves most likely represents real growth features as cells expand rapidly. Similar wobbles consistently resulted when relative elongation rate was calculated directly from groups of points along the velocity profile. The smaller peaks that formed the wobbling shape of the relative elongation curve may coincide with specialized physiological zones, such as the so-called distal elongation zone, that are sensitive to hormonal and environmental stimuli (Ishikawa and Evans, 1993, 1995; Evans and Ishikawa, 1997; Mullen et al., 1998). The wobbles could alternatively reflect the mechanics of the growth process as cells leave the meristem and enter the rapid elongation zone via an abrupt transition. During this process, cells might undergo a burst of elongation and then recover or slow before undergoing another burst.

To explore the role of ethylene in the root growth responses, we inhibited ethylene action for plants grown with high or low phosphorus. Using a similar strategy, Borch et al. (1999) previously found that ethylene limits primary root growth of beans with adequate phosphorus sufficiency but maintains root growth under phosphorus deficiency, and here, we confirm and extend these results for Arabidopsis. For most of the experiments here, we used the inhibitor of ethylene action, MCP. This inhibitor was chosen because it is a noncompetitive inhibitor and binds to the ethylene receptor tightly, thereby inactivating it (Sisler et al., 1996); consequently, the brief time needed to remove the plates for growth measurement (approximately 6 min) would vitiate the inhibition only to the extent that new receptors were synthesized. Confirmatory results with AVG suggest that there was little if any moderation of the effect of MCP because of imaging. The increased elongation rate under high phosphorus and ethylene inhibition was associated with an increased relative elongation rate in the elongation zone (Fig. 4B; Table I); in contrast, the decreased root elongation rate under low phosphorus and ethylene inhibition was associated with reduced relative elongation rate in the rapid elongation zone (Fig. 4B; Table I). These data suggest that ethylene is required for cell expansion under low phosphorus and is inhibitory under high phosphorus.

Phosphorus stress decreased the flux of epidermal cells (trichoblasts and atrichoblasts), but not of cortical cells, and ethylene helped to maintain the flux of these cell types as well as of cortical cells at low phosphorus, but only helped maintain the flux of trichoblasts at high phosphorus (Fig. 7B; Table I). Because roots elongated at a steady state, the calculated cell flux out of the growth zone equals the rate of cell production per file within the meristem (Beemster and Baskin, 1998). Cell production rate reflects the number of dividing cells in the meristem and their rate of division. In principle, either parameter could have been reduced by phosphorus stress or maintained by ethylene; however, indirect evidence implicates the number of cells rather than their division rate. Under steady-state conditions, cell division rate must be in equilibrium with relative elongation rate, otherwise cell size would progressively increase or decrease, leading to non-steady-state behavior (Green, 1976). Relative elongation rate in the meristem was not changed by phosphorus stress, and roots grew at steady state for days; consequently, we deduce that cell division rate was unchanged by phosphorus stress and that the effects of phosphorus availability and ethylene action on cell flux were mediated by the number of dividing epidermal cells.

Although cell flux was determined by analyzing only the axial dimension of root growth, it is important to realize that roots are three-dimensional and that finite cell production occurs in radial and tangential directions. Root anatomy is altered as a response to low phosphorus availability, resulting in increased files of both cortical and epidermal cells (Ma et al., 2001a). Therefore, overall cell production rate of different cell types would be different on a three-dimensional than on a simplified one-dimensional basis. Calculations of overall cell production based on changes in root anatomy (Ma et al., 2001a) and cell flux (this work) indicate that total production of cortical cells would be 8% greater than that of trichoblasts under high phosphorus, but nearly 50% greater under low phosphorus. This suggests that under phosphorus stress, some meristem initials may get recruited for increased cortical cell production, resulting in more junctions between cortical cells, which are thought to be important for root hair initiation (Masucci and Schiefelbein, 1994; Tanimoto et al., 1995; Dolan, 1996; Ma et al., 2001a).

Our present analysis focuses on root elongation, but roots also expand laterally (i.e. radially and tangentially). Lateral expansion is regulated by ethylene when roots respond to low water potential (Spollen et al., 2000) or to mechanical impedance (Sarquis et al., 1991). In view of the involvement of ethylene in regulating growth under phosphorus deficiency, reported here and elsewhere (Borch et al., 1999; Lynch and Brown, 1997), we expected that lateral expansion might have changed in response to varying phosphorus availability, particularly when ethylene was inhibited. However, for the experiment shown in Figure 1, root diameter was not significantly affected by treatment, although there was a weak positive correlation between diameter and root elongation rate (data not shown), similar to that reported previously for Arabidopsis primary roots (Van der Weele et al., 2000; Baskin et al., 2001). The constant root diameter allows analysis of the elongation data without potential complications due to simultaneous changes in lateral expansion, and indicates that controlling lat-

eral expansion does not explain ethylene's involvement in the root's response to phosphorus deficiency.

Under phosphorus stress, root hairs emerged closer to the root tip (Fig. 8; Table I), consistent with previous reports (Ma et al., 2001b; Williamson et al., 2001). In an earlier paper, we showed that the emergence of root hairs closer to the root tip acts synergistically with other morphological responses to phosphorus stress to enhance phosphorus acquisition (Ma et al., 2001b). MCP delayed the production of root hairs with high phosphorus availability, even to beyond the end of the growth zone at the higher concentration (Fig. 8), consistent with previous reports on the importance of ethylene for root hair formation (Tanimoto et al., 1995). At low phosphorus availability, however, MCP reduced the distance between the quiescent center and the first hair and increased the distance from the end of the growth zone to the first hair, so that the proportion of the growth zone that was developing root hairs was increased from 27% to 40%. The fact that the ethylene antagonist MCP has opposite effects on roots grown with high or low phosphorus availability indicates that phosphorus availability has profound effects on ethylene responsiveness.

Different strategies are required for acquisition of different resources, depending on their distribution in the soil. For example, water tends to be a "deep resource" that can be exploited by extended vertical growth of the primary root. In contrast, phosphorus is a "shallow resource" that tends to be more available in the topsoil and is therefore more readily acquired by roots that grow more superficially (Lynch and Brown, 2001). In addition, phosphorus distribution is often heterogeneous (Ryel et al., 1996), so continued soil exploration is required for plants to locate and exploit fertile soil domains. Root extension would therefore be important for soil exploration when phosphorus is limiting. Foraging for nutrients is a major function for lateral roots and accordingly the production of these roots is stimulated by phosphate deficiency (Bates and Lynch, 1996; Williamson et al., 2001; López-Bucio et al., 2002). Interestingly, phosphorus deficiency makes ethylene insensitive mutants of Arabidopsis produce even more lateral roots than wild type, whereas both genotypes have the same numbers of laterals under sufficient phosphorus, suggesting that the regulation of lateral root numbers by ethylene also depends on phosphorus status (López-Bucio et al., 2002). Considering various architectural components of the entire root system, it is possible that different root types have differential responses to hormones appropriate to their functions. It is also likely that as soil environments change, plant root systems can modify their growth and development accordingly by adjusting the balance of different hormones. It would be interesting to further examine how ethylene may affect the components of growth in lateral roots under phosphorus stress and to investigate the involvement and roles of various hormones in root growth under nutrient stress conditions by using the noninvasive method of kinematic analysis.

MATERIALS AND METHODS

Plant Culture

Seeds of Arabidopsis ecotype Columbia were obtained from the Ohio State University Arabidopsis Biological Resource Center. Seeds were surface-sterilized and sown on solidified Phytagel (Sigma-Aldrich, St. Louis) media with either high (1,000 μM) or low (1 μM) phosphorus concentrations in petri plates. The Phytagel concentration used here contains approximately 1.0 ($\pm$0.5) μM of phosphorus in the final media as determined by the phosphomolybdate method (Watanabe and Olsen, 1965). Media were prepared as previously described (Bates and Lynch, 1996; Ma et al., 2001a). Plates were wrapped with a layer of bandage tape (Micropore, 3M, St. Paul) to permit gas exchange and incubated in a plant culture room with constant light (40 μmol photons m^{-2} s^{-1}) and temperature (26°C) horizontally for 3 to 4 d until the roots reached the bottom of the plates. Plates were then placed at a 45° angle, so that subsequent root growth occurred along the bottom of the plate (Bates and Lynch, 1996; Ma et al., 2001a).

Inhibitors of Ethylene Action and Synthesis

The ethylene action inhibitor MCP (obtained as EthylBloc, containing 0.43% [w/w] MCP; Floralife Inc., Walterboro, SC), the ethylene synthesis inhibitor AVG, and the ethylene precursor ACC were used to test for the involvement of ethylene in root elongation at high and low phosphorus availability.

For experiments with MCP, plants were grown as previously described in either low or high phosphorus media. Plant culture plates were kept in separate, large, water-sealed Plexiglas growth chambers, 48 L in volume. At d 6 after germination, EthylBloc was added to a plastic weighing dish placed inside each chamber, and water was added to the dish via a syringe inserted through a rubber stopper on the roof of the chamber. MCP gas was released through the reaction of EthylBloc powder and water. Two concentrations of EthylBloc were applied: 50 and 200 mg mL^{-1} yielding concentrations of MCP in the chamber, assuming complete reaction, of 23.3 and 93.1 nL L^{-1}, respectively. Root elongation was measured every 24 h for 3 d, and MCP treatments were renewed after each measurement.

For ACC and AVG experiments, plants were grown in either low or high phosphorus media. On the 6th d of growth, 10 mL of new, liquid medium was added to the 20 mL of solid medium, being careful not to disturb the plants. The liquid medium contained the appropriate nutrient levels and AVG and ACC as desired, with the concentrations calculated based on a final volume of 30 mL. Previous work with this method verified that the contents equilibrate within 15 min (Bates and Lynch, 1996).

Root Elongation Rate

Starting at d 5 after germination, the position of the root tip was registered once each day by scoring the bottom of the petri plates at the point of the root tip with a razor blade at recorded times. This procedure was repeated subsequently until plants were 9 d old, at which time the plates were photocopied, scanned, and saved as digital files. The distance between successive marks along the root was then determined from the digitized images in Metamorph (Universal Imaging Co., West Chester, PA). The average root elongation rate for each day was calculated as the measured distance of tip movement divided by the corresponding time interval between each marking.

Imaging Root Growth for Velocity Determination

On d 5, 7, and 9 after germination, one root from each of six different plates was selected for imaging based on having near the mean growth rate as estimated by eye from the position of the root tip. Six roots from each of

the two phosphorus treatments were imaged on any given day. The plate was placed on an inverted microscope (Diaphot, Nikon, Garden City, NJ) connected to a CCD camera (XC-77, Hamamatsu Photonics, Garden City, NJ), and a series of nine images (starting from the root tip) were captured at 10-s intervals with Metamorph. A time-date generator stamped the time on each image. At the completion of capturing each stack, a background image was taken of a piece of transparent tape glued to the back of the plate. The stage was then translated to image the next segment basal of the root tip. A second stack of nine images was then captured, allowing an overlap of approximately 20% with the previous stack. This was repeated two more times until the region with mature root hairs was well into view. The background image was used to determine the overlap between adjacent stacks. The entire imaging procedure required a plate to be removed from the experimental chamber for no more than 6 min, and immediately afterward the chamber was recharged with the appropriate MCP level.

Measurement of Cell Length

After the imaging session, plates were saved for measuring the length of mature cortical cells, trichoblasts, and atrichoblasts, using Nomarski optics (×40). Twenty cells were measured on each root.

Velocity and Longitudinal Strain Rate Calculations

The analysis of root growth was one-dimensional, in the longitudinal direction only, simplifying the root as a single file of the specific type of cells under study (i.e. cortical cells, trichoblasts, or atrichoblasts). Root image stacks were processed through a novel algorithm for time sequence analysis by combining tensor analysis with a robust matching procedure, which returns confident velocity values for most pixels in the image (Jiang, 2001; Van der Weele, 2001). The algorithm finds the midline of the root and calculates the perpendicular component of velocity. Then along the perpendicular line, velocities are averaged to produce a velocity value at each pixel of the midline. A velocity output was generated for each image stack separately, and the complete root growth velocity profile was obtained by concatenating the velocity output for each stack, taking into account the overlap and tip movement between individual stacks. The final velocity profile was corrected to start from the quiescent center by subtracting the length of the root cap and was shown as a function of position along the root axis. For mathematical convenience, the quiescent center was defined as the origin, being at a spatial coordinate of $x = 0$ and nonmoving, i.e. $v = 0$. In this frame, velocity increases with distance from the quiescent center until reaching a maximum at the terminus of the growth zone.

To differentiate the velocity profile, the raw data were smoothed by an iterative, piecewise procedure, as described previously (Beemster and Baskin, 1998), and the derivative was obtained analytically from the fitted polynomials.

Because velocity in nearly all roots appeared to increase linearly for a few hundred microns before abruptly accelerating, we also used linear regression. We fitted the velocity profile to a model comprising two lines joined at a breakpoint, omitting the region at the base of the growth zone where velocity was constant. The breakpoint where the lines intersect was defined a priori as the end of the meristem, because it corresponds roughly to the position where cell division has been observed to cease (Beemster and Baskin, 1998). The slope of the line apical of the breakpoint gave the relative elongation rate within the meristem and the slope of the line basal of the breakpoint gave an average relative elongation rate for the zone of elongation. The end of the growth zone was defined as the position on the root where relative elongation rate first became zero based on the polynomial fits, and the length of the rapid elongation zone was defined as the difference between the length of the growth zone and that of the meristem. Cell flux, i.e. the rate at which cells move past a position, was determined by dividing the velocity at the base of the growth zone (i.e. maximal velocity) by mature cell length. Velocity profile and cell length were measured on the same individual roots, allowing estimation of variability of all parameters between roots.

Root Hair Initiation

From the images, the point of root hair initiation was measured as the distance between the quiescent center and the position where the first hair emerged (i.e. beyond bud stage). The distance between the first root hair and the end of the growth zone was also calculated.

Statistical Analysis

Analyses of the data were conducted using SAS (Statistical Analysis Systems Institute, 1982). ANOVA (randomized block) and Waller-Duncan K-ratio *t* test were used to compare data from different treatments. Probabilities of 0.05 or less were considered to be statistically significant.

ACKNOWLEDGMENTS

We thank Hai Jiang and Dr. Krishnan Palaniappan (University of Missouri) for generously sharing the software for quantifying the velocity profile and for help with running it, Dr. Corine M. Van der Weele (University of Missouri) for helpful discussions, and Jeff Nucciarone at the Numerically Intensive Computing Group at Pennsylvania State University for technical support.

Received August 1, 2002; returned for revision September 28, 2002; accepted November 10, 2002.

LITERATURE CITED

Baskin TI, Remillong EL, Wilson JE (2001) The impact of mannose and other carbon sources on the elongation and diameter of the primary root of *Arabidopsis thaliana*. Aust J Plant Physiol **28:** 481–488

Bates TR, Lynch JP (1996) Stimulation of root hair elongation in *Arabidopsis thaliana* by low phosphorus availability. Plant Cell Environ **19:** 529–538

Bates TR, Lynch JP (2000a) Plant growth and phosphorus accumulation of wild-type and two root hair mutants of *Arabidopsis thaliana*. Am J Bot **87:** 958–963

Bates TR, Lynch JP (2000b) The efficiency of *Arabidopsis thaliana* root hairs in phosphorus acquisition. Am J Bot **87:** 964–970

Beemster GTS, Baskin TI (1998) Analysis of cell division and elongation underlying the developmental acceleration of root growth in *Arabidopsis thaliana*. Plant Physiol **116:** 1515–1526

Bhat KKS, Nye PH (1974) Diffusion of phosphate to plant roots in soil: III. Depletion around onion roots without root hairs. Plant Soil **41:** 383–394

Bonser AM, Lynch JP, Snapp S (1996) Effect of phosphorus deficiency on growth angle of basal roots in *Phaseolus vulgaris*. New Phytol **132:** 281–288

Borch K, Bouma TJ, Lynch JP, Brown KM (1999) Ethylene: a regulator of root architectural responses to soil phosphorus availability. Plant Cell Environ **22:** 425–431

Dolan L (1996) Pattern in the root epidermis: an interplay of diffusible signals and cellular geometry. Ann Bot **77:** 547–553

Erickson RO, Sax KB (1956) Rates of cell division and cell elongation in the growth of the primary root of *Zea mays*. Proc Am Philos Soc **100:** 499–514

Evans ML, Ishikawa H (1997) Cellular specificity of the gravitropic motor response in roots. Planta **203:** S115–S122

Gahoonia TS, Nielsen NE (1997) Variation in root hairs of barley cultivars doubled soil phosphorus uptake. Euphytica **98:** 177–182

Green PB (1976) Growth and cell pattern formation on an axis: critique of concepts, terminology, and modes of study. Bot Gaz **137:** 187–202

He C, Morgan PW, Drew MC (1992) Enhanced sensitivity to ethylene in nitrogen- or phosphate-starved roots of *Zea mays* L. during aerenchyma formation. Plant Physiol **98:** 137–142

Ishikawa H, Evans ML (1993) The role of the distal elongation zone in the response of maize roots to auxin and gravity. Plant Physiol **102:** 1203–1210

Ishikawa H, Evans ML (1995) Specialized zones of development in roots. Plant Physiol **109:** 725–727

Jiang H (2001) Robust tensor-based velocity estimation of plant root growth. MS Thesis. University of Missouri, Columbia

Lewis DG, Quirk JP (1967) Phosphate diffusion in soil and uptake by plants. Plant Soil **26:** 445–453

López-Bucio J, Hernández-Abreu E, Sánchez-Calderón L, Nieto-Jacobo MF, Simpson J, Herrera-Estrella L (2002) Phosphate availability alters architecture and causes changes in hormone sensitivity in the Arabidopsis root system. Plant Physiol **129:** 244–256

Lynch JP, Brown KM (1997) Ethylene and plant responses to nutritional stress. Physiol Plant **100:** 613–619

Lynch JP, Brown KM (2001) Topsoil foraging: an architectural adaptation of plants to low phosphorus availability. Plant Soil **237:** 225–237

Ma Z, Bielenberg DG, Brown KM, Lynch JP (2001a) Regulation of root hair density by phosphorus availability in *Arabidopsis thaliana*. Plant Cell Environ **24:** 459–467

Ma Z, Walk TC, Marcus A, Lynch JP (2001b) Morphological synergism in root hair length, density, initiation and geometry for phosphorus acquisition in *Arabidopsis thaliana*: a modeling approach. Plant Soil **236:** 221–235

Masucci JD, Schiefelbein JW (1994) The *rhd6* mutation of *Arabidopsis thaliana* alters root-hair initiation through an auxin- and ethylene-associated process. Plant Physiol **106:** 1335–1346

Mullen JL, Ishikawa H, Evans ML (1998) Analysis of changes in relative elemental growth rate patterns in the elongation zone of Arabidopsis roots upon gravistimulation. Planta **206:** 598–603

Muller B, Stosser M, Tardieu F (1998) Spatial distributions of tissue expansion and cell division rates are related to irradiance and to sugar content in the growing zone of maize roots. Plant Cell Environ **21:** 149–158

Ryel RJ, Caldwell MM, Manwaring JH (1996) Temporal dynamics of soil spatial heterogeneity in sagebrush-wheatgrass steppe during a growing season. Plant Soil **184:** 299–309

Sarquis JI, Jordan WR, Morgan PW (1991) Ethylene evolution from maize (*Zea mays* L.) seedling roots and shoots in response to mechanical impedance. Plant Physiol **96:** 1171–1177

Schmundt D, Stitt M, Jahne B, Schurr U (1998) Quantitative analysis of the local rates of growth of dicot leaves at a high temporal and spatial resolution, using image sequence analysis. Plant J **16:** 505–514

Sharp RE, Silk WK, Hsiao TC (1988) Growth of the maize primary root at low water potentials: I. Spatial distribution of expansive growth. Plant Physiol **87:** 50–57

Sisler EC, Dupille E, Serek M (1996) Effect of 1-methylcyclopropene and methylenecyclopropane on ethylene binding and ethylene action on cut carnations. Plant Growth Regul **18:** 79–86

Spollen WG, LeNoble ME, Samuels TD, Bernstein N, Sharp RE (2000) Abscisic acid accumulation maintains maize primary root elongation at low water potentials by restricting ethylene production. Plant Physiol **122:** 967–976

Statistical Analysis Systems Institute (1982) SAS User's Guide: Statistics. SAS Institute, Cary, NC

Tanimoto M, Roberts K, Dolan L (1995) Ethylene is a positive regulator of root hair development in *Arabidopsis thaliana*. Plant J **8:** 943–948

Van der Weele CM (2001) A new image analysis program to measure velocity profiles for kinematic analysis of cell division and expansion in roots of *Arabidopsis thaliana*. PhD thesis. University of Missouri, Columbia

Van der Weele CM, Spollen WG, Sharp RE, Baskin TI (2000) Growth of *Arabidopsis thaliana* seedlings under water deficit studied by control of water potential in nutrient-agar media. J Exp Bot **51:** 1555–1562

Watanabe FS, Olsen SR (1965) Test of an ascorbic acid method for determining phosphorus on water and NaHCO3 extracts from soil. Soil Sci Soc Proc **29:** 677–678

Williamson LC, Ribrioux SPCP, Fitter AH, Leyser HMO (2001) Phosphate availability regulates root system architecture in *Arabidopsis*. Plant Physiol **126:** 875–882